Influence of Bulk Nematic Orientation on the Interface between a Liquid Crystalline Polymer and a Flexible Polymer

Xianfeng Li and Morton M. Denn

The Benjamin Levich Institute for Physico-Chemical Hydrodynamics, City College of the City University of New York,
New York, New York 10031
(Received 21 August 2000)

The structure of the interface between a liquid crystalline polymer (LCP) and a flexible polymer was studied using the three-dimensional bond fluctuation model in Monte Carlo simulations. Orientation in both phases in the neighborhood of the interface is sensitive to the far-field nematic orientation. The more diffuse interface caused by a homeotropic far-field orientation in the LCP results in a substantial reduction in the calculated interfacial tension relative to that for a planar far-field orientation.

The structure of a polymer/polymer interface can have a pronounced effect on macroscopic properties. While the interfacial properties of mixtures of flexible polymers have been extensively studied [1–5], the interface between an amorphous polymer and a liquid crystalline polymer (LCP), in which there is an additional length scale associated with nematic order, is unexplored. Interfacial effects resulting from the interplay of the multiple length scales can be important in polymer blends in which a small amount of an LCP is dispersed in a flexible thermoplastic polymer matrix; such blends are of considerable technological interest, because the LCP inclusions can form a fibrillar morphology during processing, leading to a "self-reinforced" composite with outstanding mechanical properties [6,7], and the LCP phase acts as a "flow modifier" during melt extrusion, causing a marked decrease in pressure drop [8].

Optical microscopy of thermotropic LCPs in the quiescent melt shows a "domain" structure, in which the correlation length for nematic order is typically a few micrometers [9]. Blends with a dispersed LCP phase in a flexible polymer matrix exhibit unusual droplet size dependence in the melt. The linear viscoelastic behavior of the blend seems to be unaffected by the interfacial tension of droplets smaller in size than the nematic correlation length, whereas larger droplets contribute to the linear viscoelasticity in the expected manner [10]. Similarly, LCP droplet relaxation following a step strain does not exhibit the size scaling observed in flexible polymer droplets in the same matrix [11].

We focus here on the effect of bulk nematic order on the structure of the interface between a LCP and a flexible polymer. We use the three-dimensional bond fluctuation model (BFM) [12] in Monte Carlo calculations, from which both the equilibrium chain conformation and the interfacial tension can be extracted. The BFM has been used to study the interfacial region between blends of flexible polymers [2–4], the dynamics of a LCP [13,14], and, of most relevance to this work, the interfacial region between polymers of different degrees of stiffness [15]. In

the framework of the model, each monomer occupies eight sites of a unit cell in a simple cubic lattice. Monomers along a chain are connected via one of 108 bond vectors, with bond lengths ranging from 2 to $\sqrt{10}$.

The amorphous polymers and LCPs are characterized in our simulations as random coils and semirigid chains, respectively, with a repulsive short-range square-well potential between unlike chain segments equal to $2.5k_BT$, where k_B is the Boltzmann constant and T is the temperature. The far-field orientation of the LCP is set by imposing a molecular orientation field. Two far-field orientations are considered here, motivated by equilibrium states in a spherical droplet of a rigid nematic [16]: a "hedgehog" structure, with a point disclination at the center, hence a homeotropic orientation in which the LCP is normal to the mean interface, and a dipolar (or "boojum") structure, with point disclinations at the poles, hence an orientation in which the LCP is parallel to the mean interface.

Only the excluded volume effect is considered for the amorphous phase, whereas two energetic interactions are also considered for the LCP phase: (i) the intrachain bending energy, equal to $E_{s0}(1 + \cos\theta_i)^2$, where θ_i is the angle between successive bonds, and (ii) the orientational energy between LCP segments and the orientation field, equal to $E_{f0}\sin^2\phi_i$, where ϕ_i is the angle between the segment and the field direction. The energetic parameters are fixed at $E_{s0} = E_{f0} = 2.5k_BT$ in the simulations reported here. The lattice dimensions are $L_x \times L_y \times L_z = 32 \times 32 \times 96$, with periodic boundaries in the x-y plane and hard walls in the z direction. The sample volume contains 800 chains with $N = 10$ monomers each, corresponding to a fraction of occupied lattice sites of 0.65. The amorphous and LCP phases occupy $\frac{1}{3}$ and $\frac{2}{3}$ of the sample volume, respectively. The chains are too short to describe entanglement dynamics in flow, but they should reflect equilibrium interfacial behavior adequately [5].

The simulation starts from an initial configuration in which the chains in both phases are random coils, corresponding to a system at infinite temperature. Following relaxation under an orientation field, the LCPs form an

organized liquid phase in which the chains tend to pack parallel to one another. Because of the extremely slow dynamics of the interfacial fluctuations, 10^8 Monte Carlo steps were required to reach equilibrium; samples were taken thereafter at every 5000th configuration in the run, and 10^4 equilibrium configurations were used in the statistics. Figures 1(a) and 1(b) show typical equilibrium configurations of the binary blend for molecular fields that orient parallel ($\phi = 0$) and orthogonal ($\phi = \pi/2$) to the interface, respectively. The LCP bulk order parameter S, defined as $\langle 3\cos^2\phi_i - 1\rangle/2$ and calculated excluding the ten lattice sites nearest the wall and the interface (located on average at the lattice position denoted 0), was 0.76 for both orientations. The calculated mass fraction profiles of the LCP along the direction normal to the interface are shown in Fig. 2. The interface is considerably broader for the homeotropic far-field orientation, where interpenetration of chain ends is less costly; for this case the interfacial region is comparable to the radius of gyration R_g of the flexible chain, which equals 3.7 in lattice units.

The orientations of chains of both types in the neighborhood of the interface are important in determining interfacial behavior. One useful measure is the asymmetry parameter, which indicates average orientation relative to a reference direction; the reference direction for the LCP is taken as the direction of the molecular field, in which case $\lambda_{n,p}$ and $\lambda_{n,h}$, the asymmetry parameters of the LCP under parallel and homeotropic orientation fields, respectively, are defined as follows [4]:

$$\lambda_{n,p} = \frac{2\langle R_x^2\rangle_z - \langle R_y^2\rangle_z - \langle R_z^2\rangle_z}{2(\langle R_x^2\rangle_z + \langle R_y^2\rangle_z + \langle R_z^2\rangle_z)}, \qquad (1a)$$

$$\lambda_{n,h} = \frac{2\langle R_z^2\rangle_z - \langle R_x^2\rangle_z - \langle R_y^2\rangle_z}{2(\langle R_z^2\rangle_z + \langle R_x^2\rangle_z + \langle R_y^2\rangle_z)}. \qquad (1b)$$
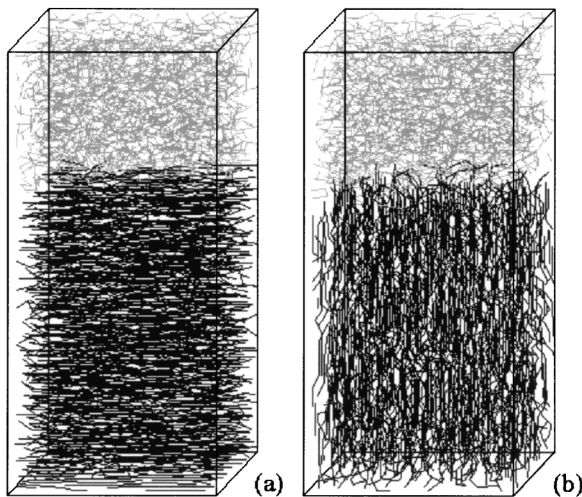
FIG. 1. Typical equilibrium configurations under (a) parallel ($\phi = 0$) and (b) homeotropic ($\phi = \pi/2$) orientation fields. The amorphous and LCP phases occupy $\frac{1}{3}$ and $\frac{2}{3}$ of the lattice, respectively.

$\langle R_s^2\rangle_z$ ($s = x, y, z$) denotes the s component of the mean-square end-to-end distance of a chain at position z. The reference direction for the flexible polymer is taken to be normal to the interface, so the asymmetry parameter λ_f is defined in the same way as $\lambda_{n,h}$. As shown in Fig. 3, there are regions of induced parallel orientation near the impenetrable walls, but they are separated from the interface by a region of bulk behavior in each phase. The semirigid chains in the bulk align along the direction of the orientation field, with $\lambda_{n,p}$ and $\lambda_{n,h}$ close to 0.9. The dramatic decrease in $\lambda_{n,h}$ to negative values within one half-chain length of the mean interface indicates a tendency of segments with a far-field homeotropic orientation to move out of plane and orient parallel to the interface; a value of -0.5 would indicate perfect orientation orthogonal to the field. There is a smaller loss of order for the chains with a far-field orientation parallel to the interface. λ_f vanishes in the bulk, reflecting the isotropy of the flexible chains, but becomes negative within about $2R_g$ of the mean interface, indicating that the flexible chains tend to orient parallel to the interface; this orientation of flexible chains is induced by the LCP phase and is greater for the planar far-field LCP orientation than for the homeotropic. The result is similar to that of Müller and Werner, who observed increasing orientation near the interface with increasing chain stiffness [15].

The interfacial tension can be obtained from the simulation using capillary wave theory [17]. The capillary fluctuation Hamiltonian [18], which reflects the free energy cost for deviations from a planar interface, is written

$$H = \int \left\{\frac{\sigma}{2}[\nabla h(\mathbf{x})]^2 + \frac{\kappa}{2}[\Delta h(\mathbf{x})]^2\right\} dx\, dy, \qquad (2)$$

where σ is the apparent interfacial tension and κ is the bending rigidity. The local interfacial position $h(\mathbf{x})$ is sampled on a lattice and can be Fourier decomposed as
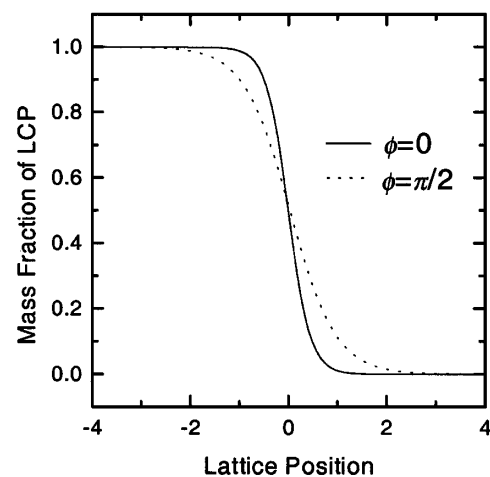
FIG. 2. Mass fraction profiles of the LCP normal to the interface.
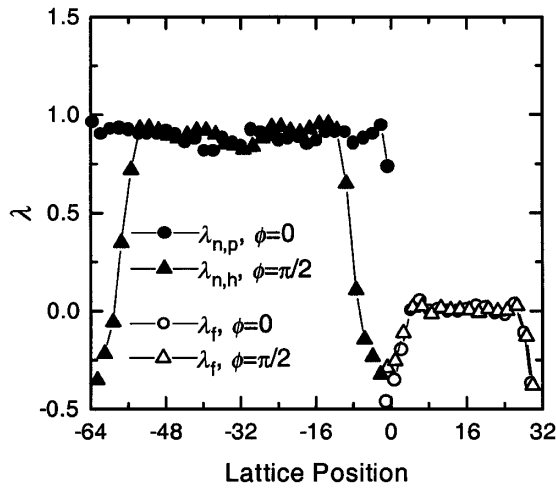
FIG. 3. Orientational asymmetry parameters for the LCP and amorphous phases for parallel and homeotropic orientations.

$$h(\mathbf{x}) = \frac{a_0}{2} + \sum_{l_x=-L_x/2}^{L_x/2} \sum_{l_y=-L_y/2}^{L_y/2} a(\mathbf{q}) \exp i\mathbf{q} \cdot \mathbf{x} \qquad (3)$$

with complex Fourier components $a(\mathbf{q})$ and wave vectors $q_x = 2\pi l_x/L_x$, $q_y = 2\pi l_y/L_y$. It then follows from the equipartition theorem that

$$\frac{2k_B T}{L_x L_y \langle a(q)^2 \rangle} = \sigma q^2 + \kappa q^4, \qquad (4)$$

where $\langle a(q)^2 \rangle$ is the mean-square value of the Fourier coefficients. The Gaussian distribution required by the quadratic Hamiltonian is shown for the first three components in Fig. 4. The data are plotted in Fig. 5 according to Eq. (4) for the two far-field orientations. The data are linear in q^2 only for the first three wave vectors; the fact that the line does not pass through the origin is probably a
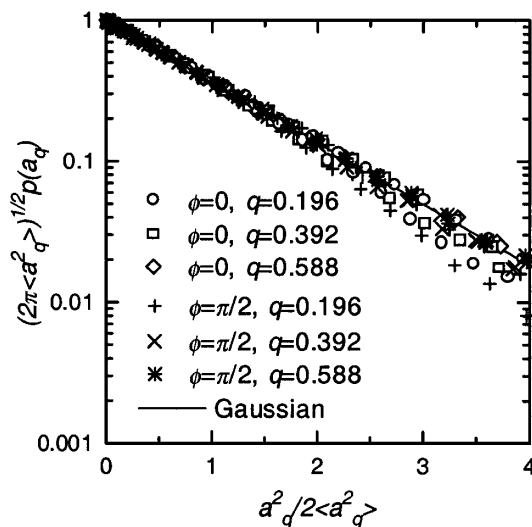
FIG. 4. Probability distribution of Fourier components of the local interfacial profiles for the three smallest wave vectors q. The solid line represents a Gaussian distribution.
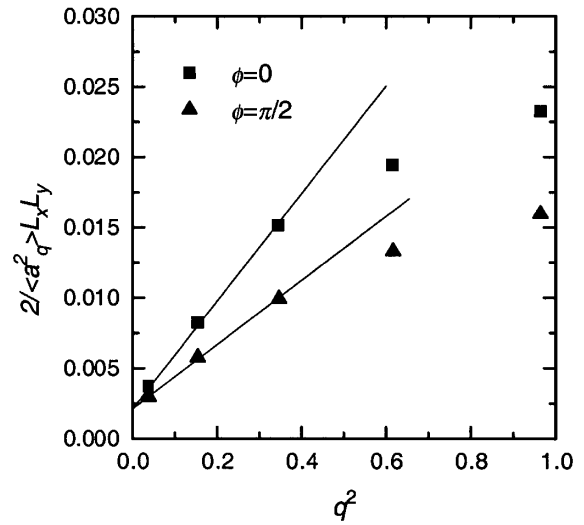
FIG. 5. Determination of the interfacial tension from the low wave vector regime of the interface profile spectrum.

reflection of the cutoff in accessible wave vectors inherent in this lattice calculation. The data in Fig. 5 show no region of positive curvature, hence no contribution from bending stiffness, which probably reflects the fact that any small curvature elasticity effect is overwhelmed by thermal fluctuations for the parameters used in this calculation. What is notable about the calculation is the large difference in slopes for the two far-field orientations. Using a value of $k_B T$ of 4.14×10^{-14} erg at room temperature and a physical lattice spacing of 2 Å [19], the calculated interfacial tensions are 3.8 and 2.3 mN/m for parallel and homeotropic orientations, respectively.

Our major conclusion is that the interface structure of incompatible blends containing a LCP and a flexible polymer is very sensitive to the far-field orientation of nematic chains. In all cases, LCP chain segments in the interfacial region tend to orient parallel to the interface and to induce a parallel orientation in the flexible chains, but this effect is greater for a parallel far-field orientation than for a homeotropic orientation; the latter is more conducive to interpenetration of chain ends. The nematic order in the far field can have a profound effect on the interfacial tension; the more diffuse interface caused by the homeotropic far field results in a calculated interfacial tension for the parameters used in these simulations that is only 60% that of the planar orientation.

[1] M. Sferrazza, C. Xiao, and R. A. L. Jones, Phys. Rev. Lett. **78**, 3693 (1997).
[2] A. Werner, F. Schmid, M. Müller, and K. Binder, J. Chem. Phys. **107**, 8175 (1997); **110**, 1221 (1999); Phys. Rev. E **59**, 728 (1999).
[3] M. Müller and M. Schick, J. Chem. Phys. **105**, 8885 (1996); A. Werner, F. Schmid, and M. Müller, J. Chem. Phys. **110**, 5370 (1999).
[4] M. Müller and M. Schick, J. Chem. Phys. **105**, 8282 (1996).

[5] M. D. Lacasse, G. S. Grest, and A. J. Levine, Phys. Rev. Lett. **80**, 309 (1998).

[6] A. A. Handlos and D. G. Baird, J. Macromol. Sci., Rev. Macromol. Chem. Phys. C **35**, 183 (1995).

[7] F. N. Cogswell, B. P. Griffin, and J. B. Rose, U.S. Patent No. 4386174 (1983); 4433083 (1984); 4438236 (1984).

[8] R. A. Weiss, W. Huh, and L. Nicolais, Polym. Eng. Sci. **27**, 684 (1987); D. Dutta, H. Fruitwala, A. Kohli, and R. A. Weiss, Polym. Eng. Sci. **30**, 1005 (1990).

[9] L. M. Walker, W. A. Kernick III, and N. J. Wagner, Macromolecules **30**, 508 (1997).

[10] H. S. Lee and M. M. Denn, J. Rheol. **43**, 1583 (1999); B. L. Riise, N. Mikler, and M. M. Denn, J. Non-Newtonian Fluid Mech. **86**, 3 (1999).

[11] H. S. Lee and M. M. Denn, J. Non-Newtonian Fluid Mech. **93**, 315 (2000).

[12] I. Carmesin and K. Kremer, Macromolecules **21**, 2819 (1988); H. P. Deutsch and K. Binder, J. Chem. Phys. **94**, 2294 (1991).

[13] A. L. Rodríguez, H. P. Wittmann, and K. Binder, Macromolecules **23**, 4327 (1990).

[14] H. D. Zhang and Y. L. Yang, Macromolecules **31**, 7550 (1998).

[15] M. Müller and A. Werner, J. Chem. Phys. **107**, 10 764 (1997).

[16] P. S. Drzaic, *Liquid Crystal Dispersions* (World Scientific, Singapore, 1995).

[17] F. P. Buff, R. A. Lovett, and F. H. Stillinger, Phys. Rev. Lett. **15**, 621 (1965); D. Beysens and M. Robert, J. Chem. Phys. **87**, 3056 (1987); A. N. Semenov, Macromolecules **27**, 2732 (1994).

[18] W. Helfrich, Z. Naturforsch. **28C**, 693 (1973); P. B. Canham, J. Theor. Biol. **26**, 61 (1970); E. Evans, Biophys. J. **14**, 923 (1974).

[19] V. Tries, W. Paul, J. Baschnagel, and K. Binder, J. Chem. Phys. **106**, 738 (1997).